PROCEEDINGS of the
23rd International Congress on Acoustics
9 to 13 September 2019 in Aachen, Germany

Influence of self-oscillating trailing edge flaplets on turbulent boundary layer – trailing edge noise.

Edward TALBOYS[(1)], Thomas F. GEYER[(2)], Christoph BRÜCKER[(1)]

[(1)]City, University of London, United Kingdom, edward.talboys.1@city.ac.uk / christoph.bruecker@city.ac.uk
[(2)]Brandenburg University of Technology, Germany, thomas.geyer@b-tu.de

Abstract

The aeroacoustics of a tripped NACA0012 aerofoil with an array of self-oscillating flexible flaplets attached to the trailing edge at low to moderate Reynolds number and at geometric angles of attack $\alpha_g = 0^\circ - 20^\circ$ is investigated. A low frequency noise reduction occurs at a chord based Strouhal number of $2 - 3$ across all Reynolds number and angles of attack. With maximum reductions reaching up to 8 dB within the Strouhal number range. This reduction is proposed to be due to a modification of the instabilities in the shear layer by the self-oscillating flaplets. A slight increase in noise level is seen at higher frequencies, however once the overall sound pressure level is calculated there is still a net overall reduction.

Keywords: Passive oscillators, aeroacoustics, trailing edge flaplets, fluid structure interaction

1 INTRODUCTION

Bio-mimicking is a topic of increasing interest within the aeroacoustic community, where many different strategies have been tested and implemented in order to reduced perceived noise levels from either aircraft, wind turbines or compressors; to name a few examples. Many of these strategies are inspired from the well-known 'silent' flight of the owl [7]. Geyer et al. [6] investigated a wide range of aerofoils with different porosities, inspired from the 'soft downy feathers' of the owl. They showed that even a small porosity showed already an aeroacoustic benefit in the low to mid frequency range, of which effect increases with increasing porosity, even in some cases reaching up to 10 dB broadband noise reduction.

Another owl-inspired technique uses trailing edge brushes or serrations, mimicking the characteristic trailing edge structure formed by the feathers of owls. Brushes have been observed to reduce noise in the high-frequency range 2–16 kHz [8], probably affecting mostly the broadband noise of the turbulent boundary layer interacting with the trailing edge. Finez et al. [4] could show that the spanwise coherence of the shed vortices in the wake behind the trailing edge is reduced by 25% in the presence of brushes. Serrations have been extensively researched in both the laminar boundary layer case [2] and turbulent boundary layer case [1]. Their mechanism in noise reduction is - similar to the brushes - through the reduction of spanwise coherence in the shed vortices. Studies with a single flexible flap at the trailing edge were investigated by Schlander and Sandberg [15]. They carried out a DNS study on a flat plate with an elastic compliant trailing edge and found an aeroacoustic benefit at low and medium frequencies with an increased noise level at the Eigen frequency of the material. These results were confirmed later by Das et al. [3] in an experimental investigation using a similar arrangement to Schlander and Sandberg [15]. Active oscillations of a trailing edge flap were studied by Jodin et al. [9]. Their investigation was focused on the wake structure and it was observed that the wake could be reduced in thickness by as much as 10%.

In the present study, a novel configuration of a flexible trailing edge is used, consisting of an array of individual elastic flaplets mimicking the tips of bird feathers aligned along the span of the wing. This type of trailing edge modification with arrays of individual mechanical oscillators in form of elastic flaps has thus far only studied by the authors [11, 10, 5]. Attached to the trailing edge of a NACA 0010 aerofoil, the rows of individual silicone flaplets clearly showed a reduction in tonal noise [10]. A follow-up study on the flow modification by this type of trailing edge was done by Talboys and Brücker [17] and demonstrated aerodynamic advantages as well.

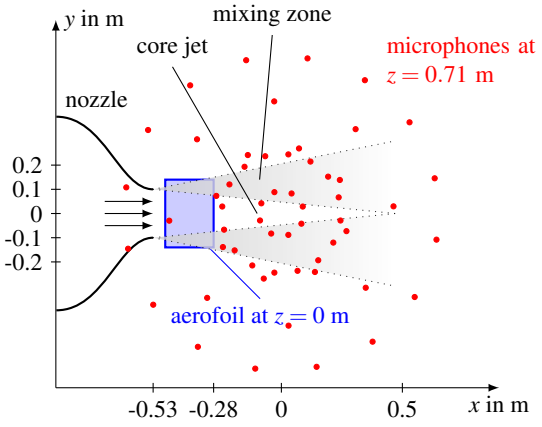

(a) Schematic display of the measurement setup (plan view)

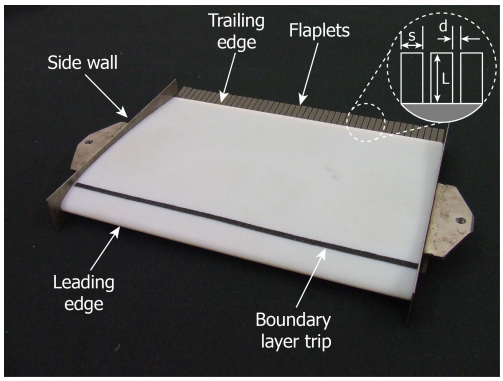

(b) Photo of the NACA 0012 aerofoil with the flaplets adhered on the trailing edge.

Figure 1. Experimental set-up

Table 1. Flaplet Dimension and Material Properties

Length (L)	Width (s)	Inter spacing (d)	Thickness	Density	Young's Modulus	Eigen frequency
20 mm	5 mm	1 mm	180 μm	1440 kg/m^3	3.12 GPa	107 Hz

Detailed High-Speed PIV measurements, coupled with simultaneous motion recordings of the flap tips, prove a stabilisation mechanism of the flaps on the boundary layer on the suction side. A lock-in was triggered by tuning the fundamental frequency of the structural bending mode of the oscillator to match with the fundamental frequency of the shear-layer on the suction side, forming regular vortex rollers in the boundary layer. This lock-in delays the growth of non-linear instabilities such as the merging of the rollers, beneficially affecting also the overall aerodynamic performance. A detailed aeroacoustic study was then carried out by Talboys et al. [18], where an untripped NACA0012 aerofoil was tested with the flaplets placed on the pressure and suction sides of the aerofoil separately, across a large range of Reynolds number and angles of attack. It was observed that when the flaplets were placed on the pressure side of the aerofoil, the laminar separation bubble was seemingly modified, due to the severe reduction in the tonal noise components of the acoustic spectra. When the flaplets were on the suction side of the aerofoil, a reduction was still seen.

2 EXPERIMENTAL ARRANGEMENT

The aerofoil used for the present study was a NACA 0012, with a chord (c) of 0.2 m and a span of 0.28 m. The model was 3D printed giving the aerofoil a trailing edge bluntness of 0.5 mm with a solid angle of 16°. The aerofoil had a boundary layer trip placed at 0.1c, such that the boundary layer was turbulent. The flexible trailing edge flaplets were manufactured, using a laser cutter, from a thin polyester film (see table 1 for dimensions and material properties). The flaplets were attached to the aerofoil using a thin strip of double sided tape, and placed such that the free ends were orientated downstream at 1.1c, allowing them to freely oscillate at their Eigen frequency in the flow field. The Eigen frequency was determined to be 107 Hz in a previous study [17], using cantilever beam theory.

Acoustic measurements took place in the small aeroacoustic open jet wind tunnel [14] at the Brandenburg University of Technology in Cottbus, with a setup similar to that used in [6]. The wind tunnel was equipped

with a circular nozzle with a contraction ratio of 16 and an exit diameter b of 0.2 m. With this nozzle, the maximum flow speed is in the order of 90 m/s and at 50 m/s, the turbulence intensity in front of the nozzle is below 0.1 %. For the present study the chord based Reynolds number was varied from 94,000 – 384,000 and the geometric angle of attack, α_g, was varied from α_g = 0° to 20°. During measurements, the wind tunnel test section is surrounded by a chamber with absorbing walls on three sides, which lead to a quasi anechoic environment for frequencies above 125 Hz.

The acoustic measurements were performed using a planar microphone array, consisting of 56 1/4th inch microphone capsules flush mounted into an aluminium plate with dimensions of 1.5 m × 1.5 m (see [12]). The microphone layout is included in Fig. 1a. The aperture of the array is 1.3 m. The array was positioned out of the flow, in a distance of 0.71 m above the aerofoil.

Data from the 56 microphones were recorded with a sampling frequency of 51.2 kHz and a duration of 60 s using a National Instruments 24 Bit multichannel measurement system. To account for the refraction of sound at the wind tunnel shear layer, a correction method was applied that is based on ray tracing [13]. The resulting microphone auto spectra and cross spectra were averaged to yield the cross spectral matrix. This matrix was further processed using the CLEAN-SC deconvolution beamforming algorithm proposed by Sijtsma [16], which was applied to a two-dimensional focus grid parallel to the array and aligned with the aerofoil.

The resulting sound pressures were then converted to sound pressure levels L_p *re* 20 μPa and 6 dB were subtracted to account for the reflection at the rigid microphone array plate.

3 RESULTS

Figure 2 shows the far field acoustic spectra, in third octave bands, for all of the test cases. For clarity, each Reynolds number test is spaced with a 20 dB increment from the previous test case. The corresponding Reynolds number can be seen adjacent to the spectra on the secondary axis. At $\alpha_g = 0°$, Fig. 2a, an interesting noise reduction can be seen in the lower frequency range (∼0.1 – 0.4 kHz). The frequency at which this reduction occurs at, increases with Reynolds number (the scaling of which will be discussed with Figures 3 and 4). Another observation is that a gain noise level at high frequency is observed for all $\mathrm{Re_c}$. When the angle of attack (α_g) is increased the low frequency benefits are still present but are reduced. The gain in the high frequency noise is also present and increases with α_g. These two features of the acoustic spectra, low frequency noise reduction and high frequency gain, has also been seen in a previous study; however in that study the boundary layer was laminar (not tripped) [18]. The findings here give further evidence to the conclusion of Talboys et al. [18] where they concluded that these differences were due to a modification of the shear layer instability on the suction side of the aerofoil by the flaplets. It should be noted here that at Reynolds numbers $<$ 121,000 at $\alpha_g = 10°$, Fig. 2b, a peak can be observed at $\sim$ 300 Hz. This is believed to be due to the relaminarisation of the boundary layer which in turn leads to the formation of laminar boundary layer tonal noise. This in itself is an interesting result as it could further confirm that the flaplets stabilise the boundary layer, as was seen in [17], as such promoting relaminarisation by locking into with the fundamental instabilities within the boundary layer and dampening out the non-linear instabilities.

A common scaling factor that is used when investigating trailing edge noise is the fifth power of the Mach number (Eqn. 1) and was first proposed in the theoretical study of Ffowcs Williams and Hall [19]. Figure 3 shows all of the test cases once they have been scaled and plotted against their respective chord based Strouhal number. The scaling works well across all Reynolds number and angles of attack. Between the Strouhal numbers of 1 and 5, the low frequency reduction can be clearly seen and at Strouhal number >20, the high frequency increase is also observed.

$$L_p^* = L_p - 10\log_{10}(M^5) \tag{1}$$

$$\Delta L_p^* = L_{p,\,\mathrm{ref.}}^* - L_{p,\,\mathrm{flaplets}}^* \tag{2}$$

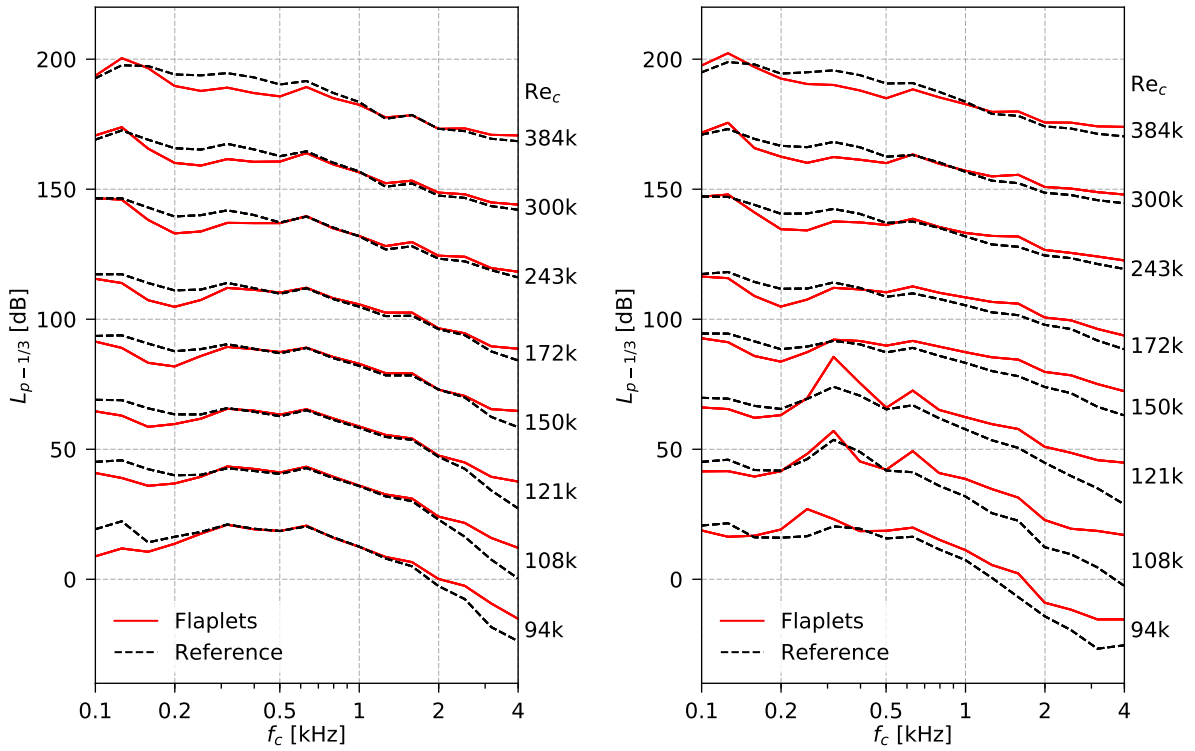

(a) $\alpha_g = 0°$

(b) $\alpha_g = 10°$

(c) $\alpha_g = 15°$

(d) $\alpha_g = 20°$

Figure 2. Comparison of the third octave sound pressure level ($L_{p\text{-}1/3}$) between the baseline aerofoil and when the flaplets are attached. Each chord based Reynolds number has had an offset of 20 dB to the previous test case for clarity. The Reynolds number of the test case can be seen on the second axis, adjacent to the spectra.

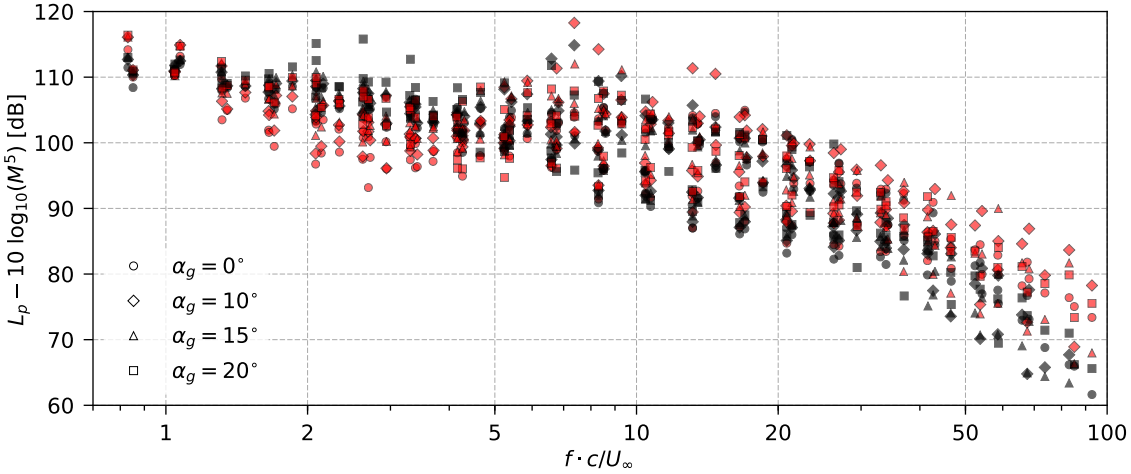

Figure 3. Third octave sound pressure levels, scaled with the fifth power of the local Mach number against the chord based Strouhal number. Points which are shaded in red indicate the cases with the flaplets and black are the reference case.

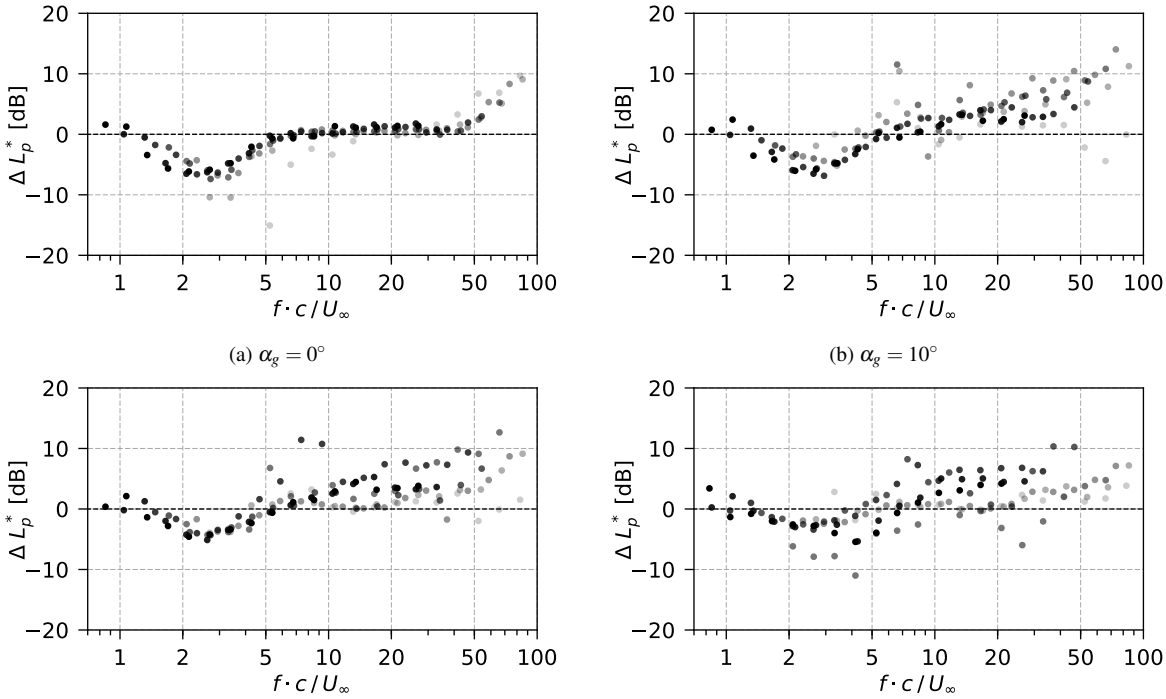

(a) $\alpha_g = 0°$ (b) $\alpha_g = 10°$

(c) $\alpha_g = 15°$ (d) $\alpha_g = 20°$

Figure 4. Difference in scaled Lp, between flaplets and reference case. The transparency of the points indicates the Reynolds number, a darker point represents a higher Reynolds number and a lighter is a lower one.

When subtracting the two scaled cases from each other, Eqn. 2, the differences become much more obvious (Figure 4). A negative value of ΔL_p^* indicates a reduction in noise level, conversely a positive value means an

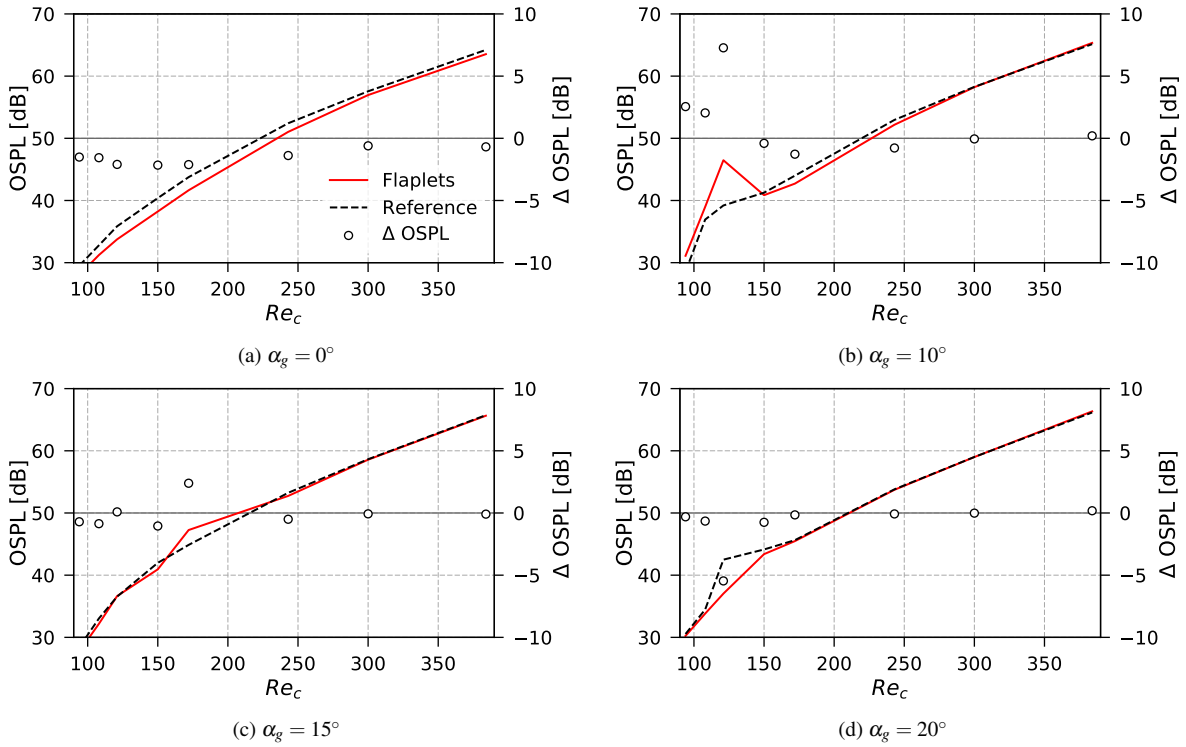

(a) $\alpha_g = 0°$ (b) $\alpha_g = 10°$

(c) $\alpha_g = 15°$ (d) $\alpha_g = 20°$

Figure 5. Overall sound pressure levels for the reference cases and with the attached flaplets. ΔOSPL has been plotted on the second axis to yield a clear indication of the difference at each Reynolds number. The zero line on the ΔOSPL axis is shown as (—)

increase. At $\alpha_g = 0°$, the test data collapse well on top of each other, very clearly showing the reduction and increase in noise levels at certain frequency bands, as previously discussed. The average maximum reduction is approximately 6 – 8 dB which occurs between a Strouhal number range of 2 – 3. Therefore, using this parameter, the frequency range at which the noise reduction occurs at can be calculated for a given Reynolds number. When the angle is increased the points start to become less correlated from one another, especially once the Strouhal number increases past 5. The noise reduction does still stay within the Strouhal number range of 2 – 4, albeit reduced, as seen in Fig.2.

To quantify the overall effect of the flaplets the overall sound pressure level has been calculated for the reference and flaplet case at each of the increments in Reynolds number. An indication of the magnitude in difference between the two aerofoils can be seen from the second axis (ΔOSPL). Figure 5a, shows that for all tested cases there is a noise reduction despite the higher frequency increase seen in Fig.2a and 4a. From the lowest Reynolds number (98,000) till Re_c = 172,000 there is an almost constant net reduction which is of the order 2 dB. As Re_c increases further the benefit approaches zero. This is thought to be due to the Eigen frequency of the flaplets being too low for the expected shedding frequency of the vortices, hence their benefit starts to become negligible. At $\alpha_g = 10°$ (Fig.5b), the relaminarisation of the boundary layer can once again be seen to have a negative effect on the acoustics. This can be seen as a sharp increase from Re_c=108,000 – 121,000. However after this point the flaplets show a slight benefit, before again converging to the same OSPL as the reference case. Increasing the angle further (Fig.5c and 5d), more or less yields an overall negligible impact on the OSPL.

4 CONCLUSIONS

This study builds off from the recent study by Talboys et al. [18] on the acoustic effect of the trailing edge flaplets when the aerofoil is subjected to a laminar boundary layer. The same low frequency benefits and high frequency increase is seen herein, and gives more indication that this effect is due to the shear layer stabilisation. At $\alpha_g = 10^\circ$ and at low Reynolds number, the flaplets seemingly cause the boundary layer to relaminarise by dampening out the non-linear instabilities in the boundary layer (as seen by Talboys and Brücker [17]). A chord based Strouhal number range of $2 - 3$ has been identified to be the range in which the maximum reduction occurs. This shows that for the current flaplet arrangement, this band of Strouhal numbers can be specifically targeted. Further investigations in order to fully quantify this effect with different flaplet properties is currently be carried out by the authors.

ACKNOWLEDGEMENTS

The position of Professor Christoph Brücker is co-funded by BAE SYSTEMS and the Royal Academy of Engineering (Research Chair no. RCSRF1617\4\11) and travel funding for Mr. E. Talboys was provided by The Worshipful Company of Scientific Instrument Makers (WCSIM), both of which are gratefully acknowledged.

REFERENCES

[1] C. Arce León, R. Merino-Martínez, D. Ragni, F. Avallone, F. Scarano, S. Pröbsting, M. Snellen, D. G. Simons, and J. Madsen. Effect of trailing edge serration-flow misalignment on airfoil noise emissions. *J. Sound Vib.*, 405:19–33, sep 2017.

[2] T. P. Chong, P. Joseph, and M. Gruber. An Experimental Study of Airfoil Instability Noise with Trailing Edge Serrations. In *16th AIAA/CEAS Aeroacoustics Conf.*, volume 332, pages 6335–6358, Reston, Virigina, jun 2010. American Institute of Aeronautics and Astronautics.

[3] C. Das, A. Mimani, R. Porteous, and C. Doolan. An experimental investigation of flow-induced noise mechanism of a flexible flat-plate trailing-edge. *Annu. Conf. Aust. Acoust. Soc.*, 5(1):1–10, 2015.

[4] A. Finez, E. Jondeau, M. Roger, and M. C. Jacob. Broadband noise reduction with trailing edge brushes. *Proc. 16th AIAA/CEAS aeroacoustics Conf.*, pages 1–13, 2010.

[5] T. F. Geyer, L. Kamps, E. Sarradj, and C. Brücker. Vortex Shedding and Modal Behavior of a Circular Cylinder Equipped with Flexible Flaps. *Acta Acust. united with Acust.*, 105(1):210–219, jan 2019.

[6] T. F. Geyer, E. Sarradj, and C. Fritzsche. Measurement of the noise generation at the trailing edge of porous airfoils. *Exp. Fluids*, 48(2):291–308, feb 2010.

[7] R. Graham. The silent flight of owls. *Aeronaut. J.*, 38(286):837–843, 1934.

[8] M. Herr. Design Criteria for Low-Noise Trailing-Edges. *13th AIAA/CEAS Aeroacoustics Conf. (28th AIAA Aeroacoustics Conf.*, pages 1–14, 2007.

[9] G. Jodin, J. F. Rouchon, J. Scheller, and M. Triantafyllou. Electroactive morphing vibrating trailing edge of a cambered wing : PIV , turbulence manipulation and velocity effects. In *IUTAM Symp. Crit. flow Dyn. Involv. moving/deformable Struct. with Des. Appl.*, Santorini, Greece, 2018.

[10] L. Kamps, C. Brücker, T. F. Geyer, and E. Sarradj. Airfoil Self Noise Reduction at Low Reynolds Numbers Using a Passive Flexible Trailing Edge. In *23rd AIAA/CEAS Aeroacoustics Conf.*, number June, pages 1–10, Reston, Virginia, jun 2017. American Institute of Aeronautics and Astronautics.

[11] L. Kamps, T. F. Geyer, E. Sarradj, and C. Brücker. Vortex shedding noise of a cylinder with hairy flaps. *J. Sound Vib.*, 388:69–84, 2016.

[12] E. Sarradj. A fast signal subspace approach for the determination of absolute levels from phased microphone array measurements. *J. Sound Vib.*, 329(9):1553–1569, 2010.

[13] E. Sarradj. A fast ray casting method for sound refraction at shear layers. *Int. J. Aeroacoustics*, 16(1-2):65–77, 2017.

[14] E. Sarradj, C. Fritzsche, T. F. Geyer, and J. Giesler. Acoustic and aerodynamic design and characterization of a small-scale aeroacoustic wind tunnel. *Appl. Acoust.*, 70(8):1073–1080, 2009.

[15] S. C. Schlanderer and R. D. Sandberg. DNS of a Compliant Trailing-Edge Flow. In *19th AIAA/CEAS Aeroacoustics Conf.*, pages 1–18, Reston, Virginia, may 2013. American Institute of Aeronautics and Astronautics.

[16] P. Sijtsma. CLEAN Based on Spatial Source Coherence. *Int. J. Aeroacoustics*, 6(4):357–374, 2007.

[17] E. Talboys and C. Brücker. Upstream shear-layer stabilisation via self-oscillating trailing edge flaplets. *Exp. Fluids*, 59(10):145, oct 2018.

[18] E. Talboys, T. F. Geyer, and C. Brücker. An aeroacoustic investigation into the effect of self-oscillating trailing edge flaplets. *J. Fluids Struct.*, (xxxx):1–13, feb 2019.

[19] J. E. F. Williams and L. H. Hall. Aerodynamic sound generation by turbulent flow in the vicinity of a scattering half plane. *J. Fluid Mech.*, 40(4):657–670, 1970.